CONF-860746--14

PREDICTIONS OF ANISOTROPIC SUPERCONDUCTIVITY IN UIr_3 AND UPt_3

T. Oguchi and A. J. Freeman

Department of Physics and Astronomy

Northwestern University, Evanston, Illinois 60201

and

G. W. Crabtree

Materials Science Division

Argonne National Laboratory,* Argonne, Illinois 60439

September 1986

jmg

CONF-860746--14

DE87 004992

Manuscript submitted to the International Conference on Anomalous Rare Earths and Actinides, July 11-17, 1986, Grenoble, France.

---

*Work supported in part by the U.S. Department of Energy, BES-Materials Sciences, under Contract #W-31-109-ENG-38

Predictions of Anisotropic Superconductivity in UIr_3 and UPt_3

T. Oguchi and A.J. Freeman
Department of Physics and Astronomy
Northwestern University
Evanston, Illinois 60201

and

G.W. Crabtree
Argonne National Laboratory
Argonne, Illinois 60439

ABSTRACT

Anisotropic singlet state superconductivity is predicted for UIr_3 (an itinerant non-heavy fermion intermetallic) as was done earlier for UPt_3 (perhaps the prototype heavy fermion system). In both, this arises from strong Uf-Xd hybridization which yields a highly anisotropic (i) Fermi surface (now confirmed by dHvA experiments of Taillefer et al. on UPt_3), (ii) electron- phonon interaction, and (iii) superconducting energy gap.

I. INTRODUCTION

Heavy fermion superconductivity - first discovered by Steglich et al.[1] in $CeCu_2Si_2$ - has attracted enormmous experimental and theoretical interest. For the uranium compounds, UPt_3 and UBe_{13}, a variety of increasingly exotic explanations has been offered to describe their seemingly unique superconducting and other properties. In sharp contrast, we have presented a consistent picture of anisotropic - but conventional (i.e., singlet state) - superconductivity in UPt_3 which explains qualitatively the gap anisotropy, the dependence of T_c on crystal perfection, the low value of the specific heat discontinuity at T_c and the induced magnetic form factor[2]. The model obtained is based on results of a fully relativistic local density band calculation for UPt_3 (which are in excellent agreement with photoemission experiments[3]) and on estimates of the strength and anisotropy of the electron-phonon interaction. The key feature is anisotropy of the superconducting energy gap which arises from the variation of the electronic mass on the Fermi surface (FS). The confirmation of our predicted FS areas and large masses by the dHvA measurements of Taillefer et al.[4], constitutes strong support and exciting verification of "a fundamental correlation between gap anisotropy and electron mass which we propose"(d)[2].

In this paper we extend our work on the FS of UPt_3 and also apply this approach to study superconductivity in UIr_3 - an itinerant non-heavy Fermion system. As in the case of UPt_3, we find a highly anisotropic FS and electron-phonon interaction which leads to a prediction of superconductivity (with a $T_c \sim 2K$) arising from strong anisotropy in the energy gap. These results also serve to emphasize the similarity between the seemingly diverse materials UPt_3 and UIr_3.

II. U-X Hybridization, Fermi Surface, and Band Masses

Unlike UPt_3 which has an hcp $MgCd_3$ structure, UIr_3 has a cubic $AuCu_3$ structure. For both - and also for URh_3, URu_3 and UPd_3 - we have employed the all-electron, fully relativistic, LMTO method with the Hedin-Lundqvist exchange and correlation potential. Systematics in hybridization between the U and X states were found and used to interpret their properties[5].

In UIr_3, E_F is located at the boundary region between the Ir-d band and the U-f band. The calculated f-projected DOS is in good agreement with the resonant photoemission experiments of Arko et al.[6]. The Fermi surface (cf. Fig. 1) has a complicated topology, due to crossing and anti-crossing of the bands. It has an M-centered electron surface connected by necks along the <100> type M-R and M-Γ lines in UIr_3. These results are qualitatively consistent with experimental and theoretical Fermi surfaces reported by Arko et al.[6]. The M-centered surfaces contain dominantly the Ir-d states while small pockets near Γ and R have moderate hybridization of the U-f and Ir-d states. It is worthwhile to note that the X- centered hole orbits on the ΓXM plane perpendicular to the <001> direction in UIr_3 have the strongest anisotropy in the f-d hybridization: 74% of U-f and 10% of Ir-d on the Γ-X lines while 2% of U-f and 89% of Ir-d on the X-M lines.

In hexagonal UPt_3, however, states which contain more Pt-d than U-f appear near H and L; the three electron surfaces around Γ have dominant U-f character. We find that hexagonal UPt_3 has stronger anisotropy in the f-d hybridization on the Fermi surface than does cubic UPt_3. It is also found that the anisotropy in UIr_3 (and URh_3!) is relatively much stronger than that in hexagonal UPt_3. This observation is contrary to expectations that

heavy fermion systems have greater anisotropy than non-heavy fermion systems.

The Fermi surface and its anisotropy plays the dominant role in determining many observed properties including anisotropic superconductivity. The successful dHvA measurements of Taillefer et al.[4] on UPt_3 add new excitement and a need for amplifying on our earlier report of its Fermi surface. Figure 2 presents Fermi surface cross sections in some principal symmetry planes. In Table 1 we give predicted values for dHvA areas (expressed as k_o radii) and (bare) band masses for these FS cross sections. For the one direction which has been measured to date, Taillefer et al. report overall good agreement with the calculated results. Significantly, the measured masses divided by the calculated masses are in about the same ratio as the average mass enhancement obtained from the measured specific heat, γ, using the calculated (bare) density of states (~ 21). This result has important significance because it supports the band model picture for the origin of superconductivity[2] in UPt_3 and, as predicted below, in UIr_3 as well.

III. Anisotropy in Electron-Phonon Interactions and Superconducting Gaps.

As was done for UPt_3, we have calculated the electron-phonon coupling, λ_{ep}, and Stoner exchange enhancement factor, S. Unlike the case of UPt_3, however, the total mass enhancement $(1 + \lambda_{tot})$ - due to electron-phonon and electron-electron interactions (such as spin fluctuations) which are not included in local density theory - are moderate in UIr_3 (and the others in the UX_3 series). From our calculated DOS and the observed specific heat we find th $\lambda_{tot} = 0.61$ for UIr_3 vs. 20 for UPt_3. The calculated S value is small (0.45)

and hence spin fluctuations are small in UIr_3 - unlike the case of UPt_3 where they are the dominant (by far) contribution to λ_{tot}.

The calculated λ_{ep} values, obtained from our band results using the rigid ion approximation, show a larger anisotropy than we obtained for UPt_3 - a result anticipated above from the more anisotropic Uf - Xd hybridization. Some calculated λ_{ep} values are given on the Fermi surface shown in Fig. 1; the strongest anisotropy on a particular orbit is found on the X-centered orbits as expected: 0.76 on the X-M lines and 0.31 on the Γ-X lines. The λ anisotropy is directly related to anisotropy in the superconducting energy gap, Δ (Ref. 7,8). Qualitative features of the gap anisotropy can be obtained in the weak anisotropy limit; we find the largest gap, 1.7 Δ, on the M-centered FS and the smallest, 0.6 Δ, on the FS near Γ (where Δ is the average gap); this anisotropy will be further enhanced by inclusion of the anisotropy of the electron-electron interaction. Interestingly, as in UPt_3, the calculated electron-phonon matrix elements from the X site are more than an order of magnitude larger than from the U site.

The calculated superconducting temperature obtained by using McMillan's equation, a μ^* of 0.13 and taking $\langle\omega^2\rangle = 1/2\ \Theta_D^2$ (where Θ_D is the Debye temperature = 225 K) and the <u>averaged</u> λ_{ep} (0.47) is T_c = 1 K; this can be considered a lower bound. Thus, superconductivity in UIr_3 is predicted to be likely - and highly anisotropic, with important consequences for such features as the specific heat at T_c, etc.

Acknowledgement

Work at Northwestern University was supported by the National Science Foundation (DMR grant No. 85-18706) and at Argonne National Laboratory by the Department of Energy. We are grateful for a computing grant on the ER CRAY.

References

1. F. Steglich et al., Phys. Rev. Lett. 43 (1979) 1892.
2. T. Oguchi and A.J. Freeman, Bull. Am. Phys. Soc. 30 (1985) 408; and J. Mag. Magn. Matls., 52 (1985) 174; and T. Oguchi, A.J. Freeman, and G.W. Crabtree, Phys. Letters (1986) in press.
3. A.J. Arko et al., Phys. Rev. Lett 53 (1984) 2050 and Bull. Am. Phys. Soc. 30 (1985) 515.
4. L. Taillefer et al., J. Mag. Magn. Matls. (1987) - this proceedings volume.
5. T. Oguchi and A.J. Freeman, J. Mag. Magn. Matls. (1986) to appear.
6. A.J. Arko, D.D. Koelling, and J.E. Schirber, in Handbook on the Physics and Chemistry of the Actinides, ed. by A.J. Freeman and G.W. Lander (North-Holland, Amsterdam, 1984) vol. 2, p. 175.
7. W.H. Butler and P.B. Allen, Superconductivity in d- and f-band metals (D.H. Douglass, ed., Plenum Press, 1976) p. 73.
8. M. Peter, J. Ashkenazi, and M. Dacorogna, Helv. Phys. Acta., 50, 267 (1977).

FIGURE CAPTIONS

Fig. 1. Fermi surface of cubic UIr_3 in some high symmetry planes.

Fig. 2. Fermi surface cross sections for hcp UPt_3 showing the 3 electron surfaces around Γ and the two hole surfaces around the outer regions of the Brillouin zone.

Table 1. Predicted areas given as effective radii, k_o (in $\mathring{A}^{-1}$) and effective masses (in free electron mass units) for the FS cross sections shown in Fig. 2. There is also a K3 orbit in the KKHH ($\perp \hat{k}y$), not given below, with $k_o = 0.188$ and $m^* = 2.1$.

ΓMLA			ΓKHA			ΓMK($\perp k_z$)			ALH($\perp k_z$)			MKHL($\perp \hat{k}_x$)		
orbit	k_o	m*	orbit	k_o	m*	orbit	k_o	m*	orbit	k_o	m*	orbit	k_o	m*
Γ1	0.072	1.3	Γ1	0.070	1.2	Γ1	0.102	1.7	A4	0.206	2.2	ML4	0.048	0.8
Γ2	0.219	2.5	Γ2	0.225	3.2	Γ2	0.140	1.5	A4	0.454	4.6	ML4	0.058	1.3
Γ3	0.366	4.2	Γ3	0.419	6.1	Γ3	0.356	5.1	A5	0.217	2.3	K3	0.190	2.4
L4	0.119	1.0	K3	shared with MKHL		K3	0.203	2.4	A5	0.422	2.8			
L4	0.375	6.2	AH4	0.155	1.4									
ML4	0.041	0.9	AH5	0.082	0.8									
AL5	0.100	0.7												

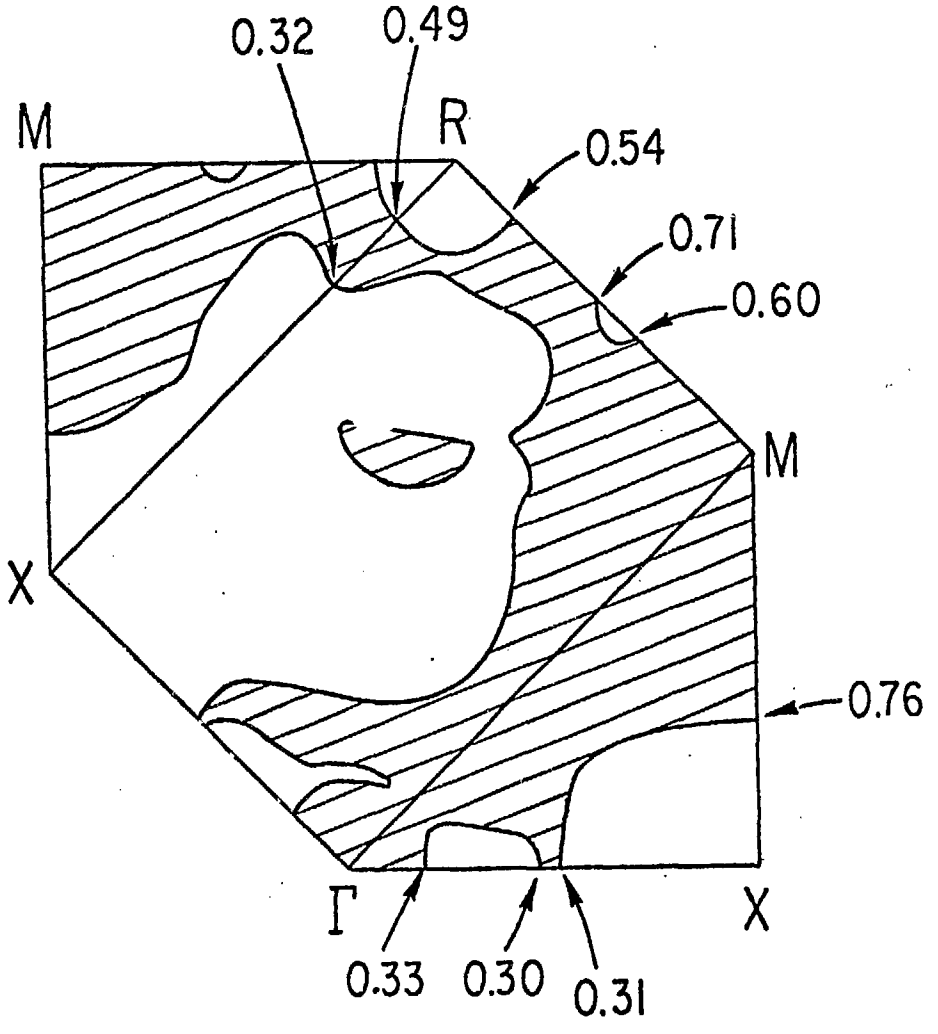
0.32
0.49
M
R
0.54
0.71
0.60
M
X
0.76
Γ
X
0.33
0.30
0.31

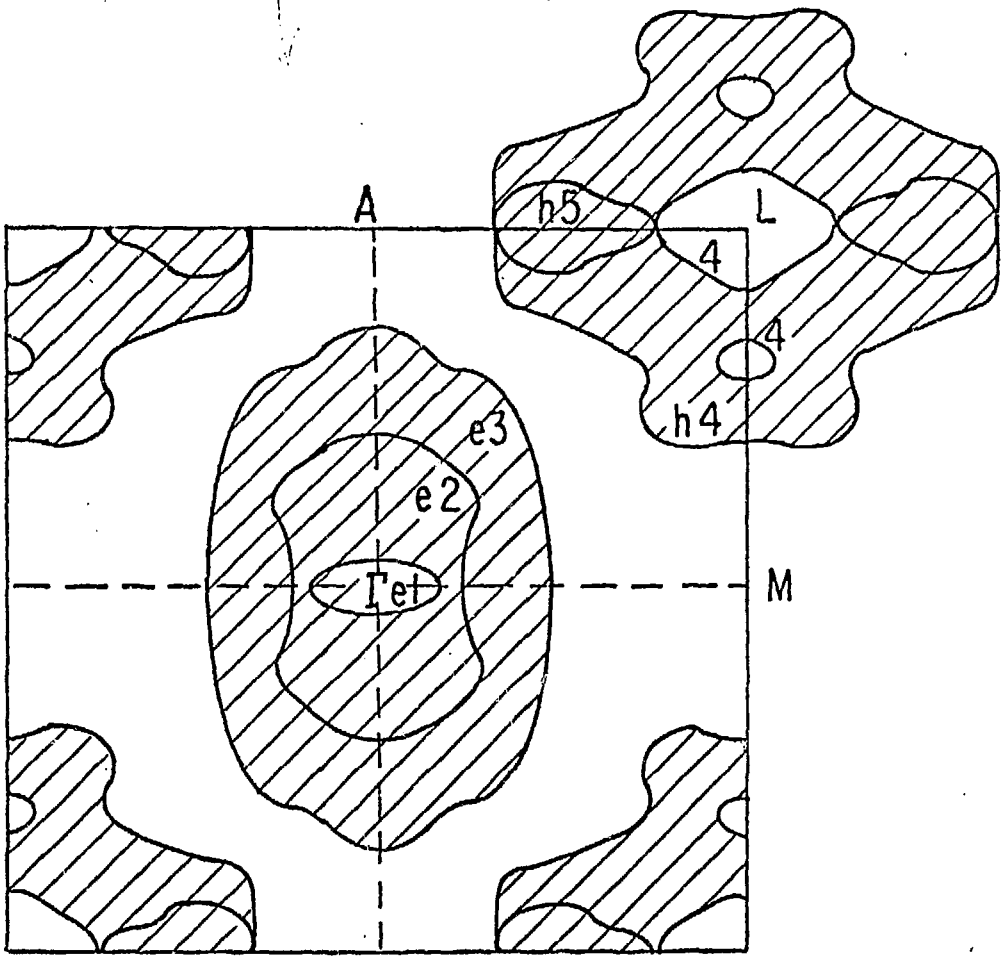
A
h5
L
4
4
h4
e3
e2
Γet
M

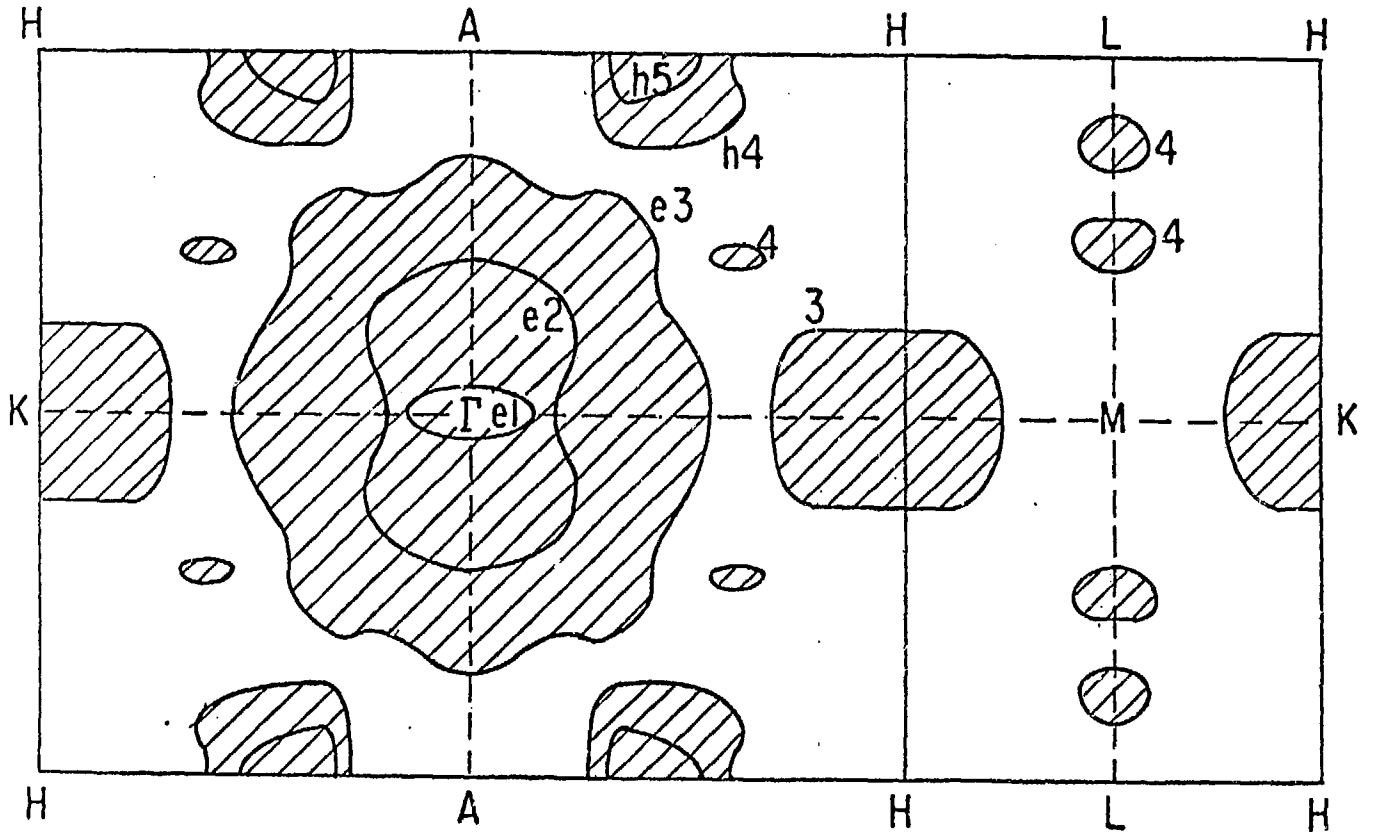
H
A
H
L
H
h5
h4
4
4
e3
4
e2
3
K
Γ e1
M
K
H
A
H
L
H

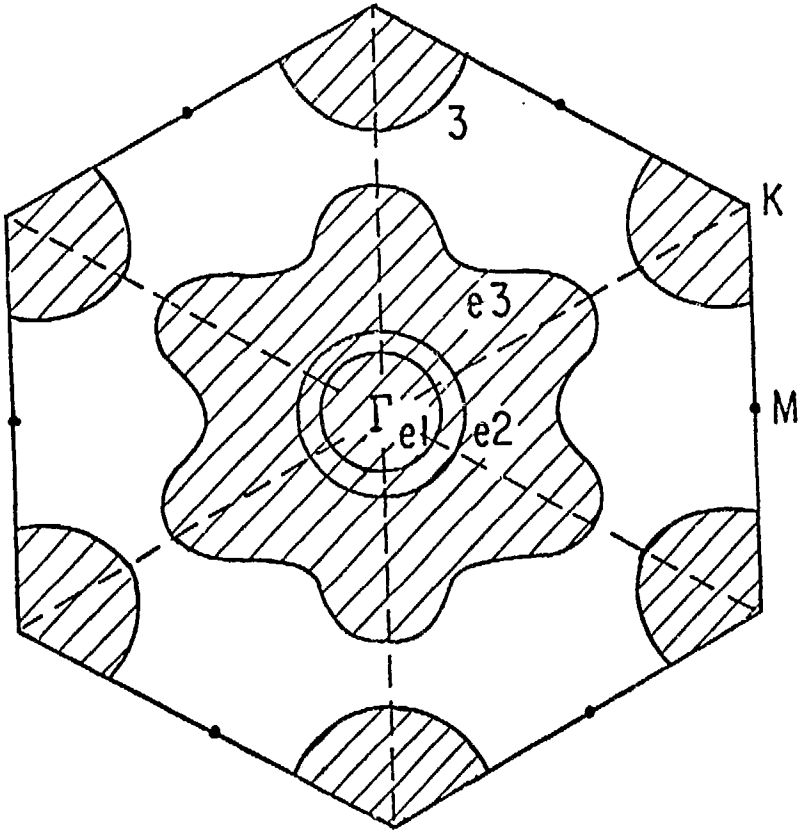
3
K
e3
M
Γ
e1
e2

(21)

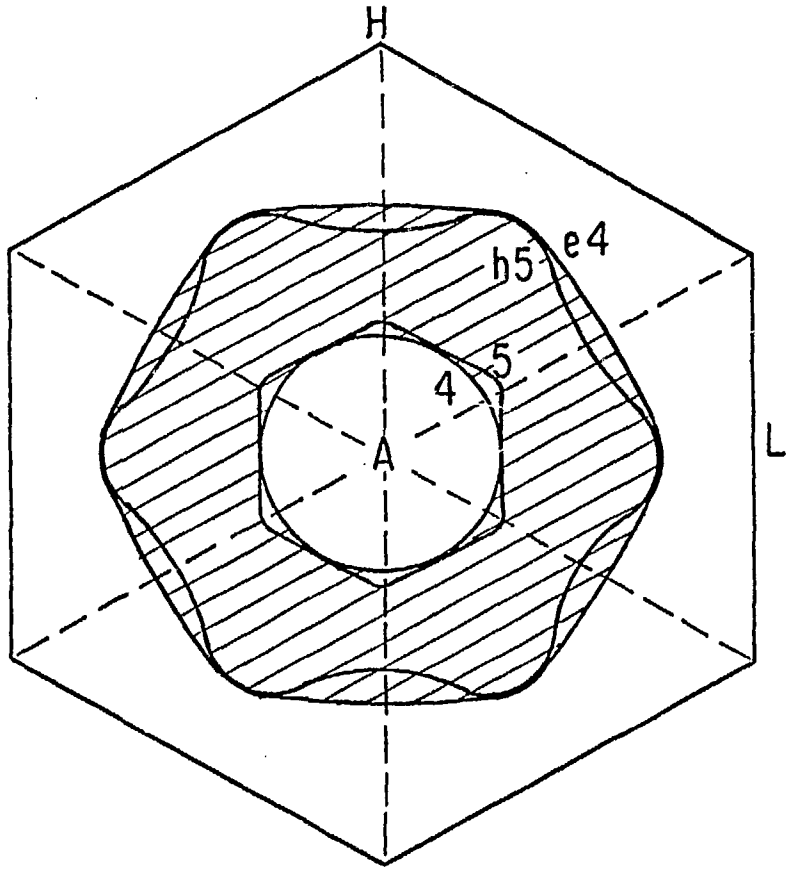

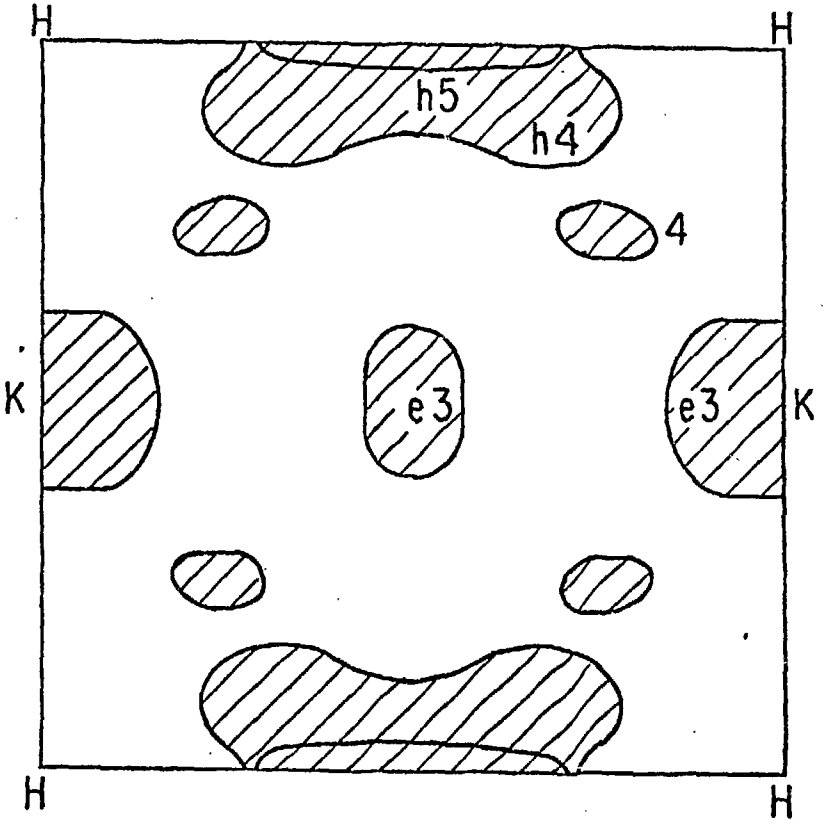
H
H
h5
h4
4
K
e3
e3
K
H
H